

# ON MODELLING OF DELAMINATION IN LAMINATED PLATES (AN ALTERNATIVE TO FRACTURE MECHANICS APPROACH)

J. N. Reddy\*, A. Grimaldi\*\* and D. Frederick\*

*\*Department of Engineering Science and Mechanics, Virginia Polytechnic Institute and State University, Blacksburg, VA 24061, USA*

*\*\*Faculty of Engineering, Second University of Rome, Italy*

## ABSTRACT

The unilateral contact approach is used to model the initial debonding and subsequent delamination of two-layer or multi-layer symmetric laminated plates under transverse loads. The mathematical formulation of the approach and associated finite element model are presented. The bond material (or adherent) is modelled as a continuum that has a uniaxial (in the transverse direction) elastic response. The flexural behavior of the plate is modelled by means of the Hencky-Mindlin type shear deformation theory. Two sample problems are presented. The relationship between the brittle fracture mechanics approach and the present approach is also discussed.

## KEY WORDS

Delamination, finite elements, fracture mechanics approach, laminated plates, shear deformation theory, symmetric laminates, transverse load, unilateral contact approach.

## INTRODUCTION

Plates laminated of orthotropic layers are increasingly used in aerospace, civil, and mechanical engineering structures. This is because by selecting the lamination scheme the designer can tailor the strength and stiffness of laminates. If the edges of laminates are not secured properly, delamination of the layers at the edges can take place during service conditions. The delamination can occur either due to the presence of transverse normal tensile stress or due to imperfect bonding between layers. In the latter case, the delamination propagates under applied loads, especially if these loads are transverse to the laminate. The present study deals with the modelling of the delamination growth using the unilateral contact approach (Signorini, 1933; Fichera, 1972; Duvrant and Lions, 1976; Fremond, 1982; Toscano and Maceri, 1980; Grimaldi and Reddy, 1982; Ascione and Grimaldi, 1984).



## THEORETICAL MODEL

In the present study we assume that the plate under consideration is laminated of two identical layers or several layers such that the lamination is symmetric about the midplane of the laminate. Further, we assume that the initial delamination is at an edge of the midplane. Because of the assumed symmetry, we can model the delamination of the upper half laminate from the midplane (see Fig. 1a).

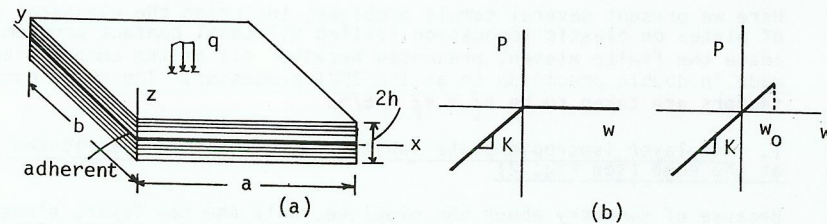


Fig. 1. Laminated plate geometry and the load-deflection relations for the adherent material

## LAMINATE THEORY

Consider a plate of uniform thickness  $h$  composed of a finite number of orthotropic layers with arbitrary orientations with respect to the plate coordinate system. The coordinate system is chosen such that the  $x$ - $y$  plane coincides with midplane,  $R$ , and the  $z$ -axis is normal to the middle plane.

The displacement field in the shear deformable theory is given by (Whitney and Pagano, 1970; Reddy, 1980)

$$\begin{aligned} u(x, y, z) &= u_0(x, y) + z\phi_x(x, y) \\ v(x, y, z) &= v_0(x, y) + z\phi_y(x, y) \\ w &= w(x, y) \end{aligned} \quad (1)$$

where  $u$ ,  $v$ , and  $w$  are the displacements along  $x$ ,  $y$  and  $z$  directions respectively,  $u_0$  and  $v_0$  are the in-plane displacements of the middle plane, and  $\phi_x$  and  $\phi_y$  are the rotations about the  $y$  and  $x$  axes, respectively.

The equilibrium equations of the plate can be obtained using the principle of virtual displacements (Reddy, 1980)

$$\begin{aligned} N_{1,x} + N_{6,y} &= 0, \quad N_{6,x} + N_{2,y} = 0 \\ Q_{1,x} + Q_{2,y} + q &= P(w) \\ M_{1,x} + M_{6,y} - Q_1 &= 0, \quad M_{6,x} + M_{2,y} - Q_2 = 0 \end{aligned} \quad (2)$$

where  $w_{,x} = \partial w / \partial x$ , etc.,  $q$  is the distributed transverse load,  $P$  is the reaction of the adherent, and  $N_i$ ,  $Q_i$ , and  $M_i$  are the stress and moment resultants defined by

$$(N_i, M_i) = \int_{-h/2}^{h/2} (1, z) \sigma_i dz, \quad (Q_1, Q_2) = \int_{-h/2}^{h/2} (\tau_{xz}, \tau_{yz}) dz. \quad (3)$$

Here  $\sigma_i$  ( $i = 1, 2, 6$ ) denote the in-plane stress components ( $\sigma_1 = \sigma_x$ ,  $\sigma_2 = \sigma_y$ , and  $\sigma_6 = \sigma_{xy}$ ).

Assuming monoclinic behavior (i.e., existence of one plane of elastic symmetry) for each layer, the constitutive equations for an arbitrarily laminated plate can be expressed as

$$\begin{Bmatrix} N_i \\ M_i \end{Bmatrix} = \begin{bmatrix} A_{ij} & B_{ij} \\ B_{ji} & D_{ij} \end{bmatrix} \begin{Bmatrix} \epsilon_j^0 \\ \kappa_j \end{Bmatrix}, \quad \begin{Bmatrix} Q_1 \\ Q_2 \end{Bmatrix} = \begin{bmatrix} A_{55} & A_{45} \\ A_{45} & A_{44} \end{bmatrix} \begin{Bmatrix} \gamma_{xz} \\ \gamma_{yz} \end{Bmatrix} \quad (4)$$

where

$$\epsilon_1^0 = u_{0,x}, \quad \epsilon_2^0 = v_{0,y}, \quad \epsilon_6^0 = u_{0,y} + v_{0,x}, \quad \gamma_{xz} = w_{,x} + \phi_x, \quad (5)$$

$$\kappa_1 = \phi_{x,x}, \quad \kappa_2 = \phi_{y,y}, \quad \kappa_6 = \phi_{x,y} + \phi_{y,x}, \quad \gamma_{yz} = w_{,y} + \phi_y$$

The plate stiffnesses  $A_{ij}$ ,  $B_{ij}$ , and  $D_{ij}$  are given by

$$(A_{ij}, B_{ij}, D_{ij}) = \sum_m \int_{z_m}^{z_{m+1}} Q_{ij}^{(m)}(1, z, z^2) dz, \quad (i, j = 1, 2, 6), \quad (6)$$

$$A_{ij} = \sum_m \int_{z_m}^{z_{m+1}} k_\alpha k_\beta Q_{ij}^{(m)} dz, \quad (\alpha = 6-i, \beta = 6-j, i, j = 4, 5). \quad (7)$$

where  $Q_{ij}^{(m)}$  are the material coefficients of the  $m$ -th layer in the plate coordinates,  $z_m$  is the distance from the mid-plane to the lower surface of the  $m$ -th layer, and  $k_i$  are the shear correction coefficients.

For the symmetrically laminated plates, all  $B_{ij}$  are zero and  $A_{16} = A_{26} = D_{16} = D_{26} = A_{45} = 0$ . Consequently, the coupling between  $(u_0, v_0)$  and  $(w, \phi_x, \phi_y)$  (i.e. bending-stretching coupling) vanishes. Therefore, in the remaining discussion we will not consider the inplane displacements. Then the moment and shear force results can be expressed in terms of the generalized displacements as

$$\begin{aligned} M_1 &= D_{11} \frac{\partial \phi_x}{\partial x} + D_{12} \frac{\partial \phi_y}{\partial y}, \quad M_2 = D_{12} \frac{\partial \phi_x}{\partial x} + D_{22} \frac{\partial \phi_y}{\partial y} \\ M_6 &= D_{66} \left( \frac{\partial \phi_x}{\partial y} + \frac{\partial \phi_y}{\partial x} \right), \quad Q_1 = A_{55} \left( \frac{\partial w}{\partial x} + \phi_x \right), \quad Q_2 = A_{44} \left( \frac{\partial w}{\partial y} + \phi_y \right). \end{aligned} \quad (8)$$

The reaction force  $P$  of the bond material, which is treated as an elastic foundation, can be expressed as

$$P(w) = K(w) \cdot w \quad (9)$$

where  $K(w)$  is, in general, a nonlinear function of the displacement and is a property of the bonding material. In the present study we will consider



cases in which  $K$  is a finite constant. Figure 1b contains two cases of the load-deflection relationship. In the first case, the modulus is bilinear with  $K \neq 0$  in compression and  $K = 0$  in tension. In the second case, the modulus is linear but allowed to have only finite tensile strength (or finite deflection  $w_0$  in tension).

#### FINITE-ELEMENT MODEL

The finite-element model of Eqs. (2)-(8) can be derived by assuming interpolation of the form (Reddy, 1984)

$$w = \sum_{i=1}^n w_i \psi_i, \quad \psi_x = \sum_{i=1}^n X_i \psi_i, \quad \psi_y = \sum_{i=1}^n Y_i \psi_i \quad (10)$$

over an element  $R^e$ . Substituting Eq. (10) into the virtual work statement associated with the equations, we obtain

$$\begin{bmatrix} [K^{11}] & [K^{12}] & [K^{13}] \\ & [K^{22}] & [K^{23}] \\ \text{symm.} & & [K^{33}] \end{bmatrix} \begin{Bmatrix} \{w\} \\ \{X\} \\ \{Y\} \end{Bmatrix} = \begin{Bmatrix} \{F^1\} \\ \{F^2\} \\ \{F^3\} \end{Bmatrix} \quad (11)$$

where

$$[K^{11}] = [\bar{K}^{11}] + [\hat{K}^{11}],$$

$$\bar{K}_{ij}^{11} = \int_{R^e} (A_{55} \frac{\partial \psi_i}{\partial x} \frac{\partial \psi_j}{\partial x} + A_{44} \frac{\partial \psi_i}{\partial y} \frac{\partial \psi_j}{\partial y}) dx dy, \quad \hat{K}_{ij}^{11} = \int_{R^e} K(w) \psi_i \psi_j dx dy$$

$$K_{ij}^{12} = \int_{R^e} A_{55} \frac{\partial \psi_i}{\partial x} \psi_j dx dy, \quad K_{ij}^{13} = \int_{R^e} A_{44} \frac{\partial \psi_i}{\partial y} \psi_j dx dy$$

$$K_{ij}^{22} = \int_{R^e} (D_{11} \frac{\partial \psi_i}{\partial x} \frac{\partial \psi_j}{\partial x} + D_{66} \frac{\partial \psi_i}{\partial y} \frac{\partial \psi_j}{\partial y} + A_{55} \psi_i \psi_j) dx dy$$

$$K_{ij}^{23} = \int_{R^e} (D_{12} \frac{\partial \psi_i}{\partial x} \frac{\partial \psi_j}{\partial y} + D_{66} \frac{\partial \psi_i}{\partial y} \frac{\partial \psi_j}{\partial x}) dx dy,$$

$$K_{ij}^{33} = \int_{R^e} (D_{66} \frac{\partial \psi_i}{\partial x} \frac{\partial \psi_j}{\partial x} + D_{22} \frac{\partial \psi_i}{\partial y} \frac{\partial \psi_j}{\partial y} + A_{44} \psi_i \psi_j) dx dy$$

$$F_i^1 = \int_{R^e} q \psi_i dx dy + \int_S Q_n \psi_i ds, \quad Q_n = Q_1 n_x + Q_2 n_y$$

$$F_i^2 = \int_S M_n \psi_i ds, \quad M_n = M_1 n_x + M_6 n_y$$

$$F_i^3 = \int_S M_{ns} \psi_i ds, \quad M_{ns} = M_6 n_x + M_2 n_y. \quad (12)$$

The element stiffness matrix in (11) is of the order  $3n$  by  $3n$ , where  $n$  is the number of nodes per element. For example, when the four-node rectangular element is used, then the element stiffness matrix is of the order 12 by 12.

The element equations in (11) can be assembled, boundary conditions can be imposed, and the equations can be solved in the usual manner (Reddy, 1984). As is well known among researchers working with the Mindlin plate element, reduced integration of the shear energy (i.e., coefficients of  $A_{44}$  and  $A_{55}$ ) is necessary to obtain accurate results. We shall investigate this effect in the numerical examples to be discussed next.

#### NUMERICAL EXAMPLES

Here we present several sample problems, including the classical problems of plates on elastic foundation (called bilateral contact problems) to validate the finite element presented herein. All of the computations were made in double precision on an IBM 3081 processor. The shear correction factors are taken to be  $k_1^2 = k_2^2 = 5/6$ .

##### 1. Two-layer isotropic plate subjected to symmetric distributed line load at the edge (see Fig. 2)

Because of symmetry about the midplane, only the top layer, along with the bond material, is modeled using uniform meshes of  $1 \times 8$  four-node elements and  $1 \times 4$  mesh of nine-node elements. The following parameters were used:

$$\frac{a}{b} = 8, \quad \frac{a}{h} = 16, \quad \frac{E}{K} = 10^2, \quad \nu = 0.1 \quad (13)$$

Table 1 contains the nondimensionalized deflection versus the distance along the long side. The analytic solution (from [11]) is compared with the finite-element solution with full and reduced integrations. Full integration means the usual integration ( $2 \times 2$  for the linear element and  $3 \times 3$  for the quadratic element) and reduced integration means one order less than the usual. In Table 1, R refers to the integration scheme in which full integration is used to evaluate the bending stiffness and reduced integration is used to evaluate the shear stiffness, and F refers to the integration scheme in which full integration is used to evaluate both the bending and shear stiffnesses. From the results it is clear that, in general, reduced integration gives the best results. It is also clear that refined meshes and higher-order elements are less sensitive to the integration order than coarse meshes and linear elements. The finite element solution is in good agreement with the analytical solution, which is based on the classical theory of infinite beams on elastic foundation.

Table 1 Comparison of the dimensionless transverse deflections ( $w = wD \times 10^3 / q_0 a^4$ ) for the rectangular plate of Problem 1

$x/a$	Analytical solution	Finite Element Solution			
		4-Node(F)	4-Node(R)	9-Node(F)	9-Node(R)
0.000	20.188	16.552	19.993	20.154	20.367
0.125	12.563	11.601	12.553	12.650	12.691
0.250	6.500	7.296	6.499	6.635	6.498
0.375	2.375	3.901	2.341	2.440	2.269
0.500	0.001	1.397	0.100	-0.015	-0.043
0.625	-1.075	-0.394	-1.283	-1.218	-1.204
0.750	-1.35	-1.712	-1.704	-1.670	-1.622
0.875	-1.55	-2.786	-1.762	-1.741	-1.719
1.000	-1.54	-3.782	-1.704	-1.713	-1.715

##### 2. One-dimensional delamination of a two-layer isotropic plate subjected to a distributed line load at the edge (Fig. 3)



This problem is similar to one considered above, except that initially there is debonding at the edge  $x = 0$  for all  $y$ , and the strength of the bonding material (i.e., adherent) is finite. Let the initial length of the delamination be  $\ell_0$ , and let  $\gamma$  be the surface energy per unit area (of opening). We first use the fracture mechanics approach (mode I of fracture) to determine the load-delamination relationship.

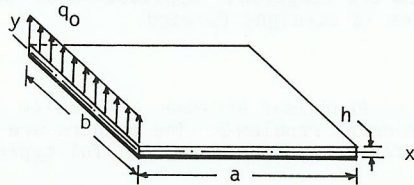


Fig. 2. Rectangular plate on elastic foundation

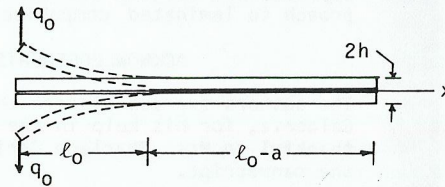


Fig. 3. Delamination in a two-layer plate

The delamination propagates when the energy release equals the surface energy  $G$ :

$$G = \gamma b \quad (14)$$

where  $G$  is the energy release per unit length of opening, which is given by

$$G = -\frac{d\Pi}{d\ell} \quad (15)$$

$\Pi$  being the total potential energy, and  $d\ell$  is the infinitesimal length along the opening. The total potential energy for the problem at hand is equal to the work done by the applied load,

$$\Pi = -\frac{1}{2}(\text{force})(\text{displ.}) = -\frac{q_0^2 \ell^3 b}{6D} \quad (\ell > \ell_0) \quad (16)$$

From Eqs. (14) - (16) we have

$$\ell = \frac{\sqrt{2DY}}{q_0} \quad (\ell > \ell_0) \quad (17)$$

which gives the length  $\ell$  of delamination as a function of the distributed load  $q_0$ . The load-deflection relation is given by Grimaldi and Reddy, (1982)

$$Q = \begin{cases} \frac{W}{\xi_0^3}, & \ell = \ell_0 \quad (\xi_0 = \ell_0/L) \\ \frac{1}{\sqrt{W}}, & \ell > \ell_0 \end{cases} \quad (18)$$

$$L = \sqrt{2D/\gamma}, \quad Q = q_0/\gamma, \quad W = \frac{3}{2} \frac{W}{L}, \quad \xi = \ell/L \quad (19)$$

This completes the derivation of the analytical solution.

<sup>1</sup>The delaminated part of the plate is treated as a cantilever of length  $\ell$ , flexural rigidity  $Db$ , and force  $q_0 b$  at the free end.

In the present (i.e., unilateral contact) approach, the initial delamination is modeled by setting  $K = 0$  in the elements that are used between  $x = 0$  and  $x = \ell_0$ . The new delamination length,  $\ell$ , is determined by checking the strain energy of the adherent against allowable energy  $\gamma$  for the material. When the strain energy of the adherent exceeds the allowable value, then the element is assumed to be delaminated. Of course, for accurate prediction of the delamination length, the elements in the vicinity of the opening should be small enough (at least equal to the wave length,  $\lambda^4 = 4D/K$ ). The energy  $\gamma$  can be related to the allowable deflection  $w_0$  by using  $\gamma = \text{strain energy} = (1/2)Kw_0^2$ ,

$$w_0 = \sqrt{\frac{2\gamma}{K}}. \quad (20)$$

The following iterative scheme is used in the finite element analysis:

- (i) Begin with the initial length  $\ell_0$  of the opening, and identify an interval,  $\ell_0 < x < \ell_0 + 5\lambda$ , in which the mesh is refined.
- (ii) Solve the finite element equations for specified  $W$  at the edge  $x = 0$ .
- (iii) Check to see if the deflection  $w$  at  $x = \ell_0$  is greater than the critical deflection,  $w_0$ . If no, no delamination occurred.
- (iv) If  $w > w_0$ , delamination occurred. Then the first element in the interval,  $\ell_0 < x < \ell_0 + 5\lambda$ , is assumed to have delaminated, and compute the reaction force  $Q$  there. Then, reconstruct the finite element mesh with the new delamination length  $\ell_1$  (see Fig. 4), and repeat steps (ii) and (iii).

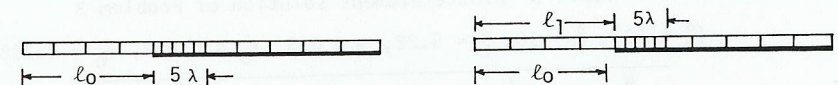


Fig. 4. Finite element mesh for the delamination problem of Fig. 3

Table 2 contains the results of the finite-element analysis and the analytical solution (18) of the fracture mechanics approach. In Table 2,  $N_T$  denotes the total number of elements and  $N_R$  denotes the number of elements in the interval of length  $5\lambda$ . The finite element solution based on the unilateral contact approach is in good agreement with the analytical solution. A complete agreement cannot be expected because, Eq. (20) is valid

Table 2 Comparison of the finite element solution with the analytical solution of Problem 2  
( $a/h = 10^5$ ,  $a/b = 10$ ,  $\nu = 0.3$ ,  $a/\lambda = 2 \times 10^3$ ,  $\xi_0 = 0.78$ )

W	Analytical Eq. (18)		Finite Element			
	$\xi$	Q	$N_T = 20$ , $\xi$	$N_R = 15$ , Q	$N_T = 40$ , $\xi$	$N_R = 30$ , Q
0.5	0.783	1.04	0.783	0.987	0.783	0.984
1.0	1.000	1.000	0.981	1.087	0.987	0.989
5.0	2.236	0.447	2.218	0.420	2.223	0.419
10.0	3.160	0.316	3.122	0.304	3.153	0.307



in the limiting case of  $K \rightarrow \infty$  and  $\lambda \rightarrow 0$ . Figure 5 contains the plots of  $Q$  versus  $W$ , and  $\xi$  versus  $W$ , as obtained by the two approaches.

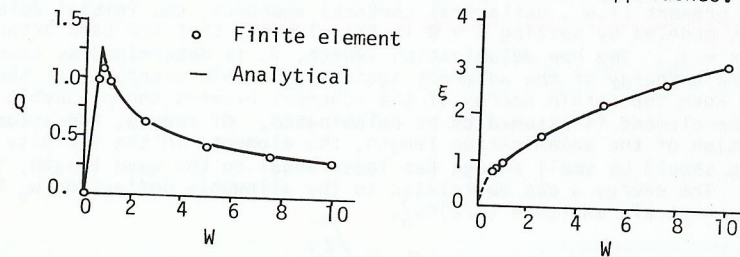


Fig. 5. Plots of  $W$  versus  $Q$  and  $\xi$  for the two-layer plate in Prob. 2

### 3. Two-dimensional delamination of a two-layer square plate

Here we consider a more general (and difficult) problem than one considered above. We assume that the delamination begins from a corner of the plate and propagates in the midplane of the laminate (see Fig. 6a).

We assume that the initial delamination area is a square of length  $l_0$ , as shown in Fig. 6b. The mesh in the region beyond the initial square area but within five wavelengths distance is refined. The delaminated new area and finite element mesh are shown in Fig. 6c. We use the iterative procedure described earlier to determine  $Q = P/\gamma L$ ,  $\xi = l_x/L$ , and  $\eta = l_y/L$ . The results are presented in Table 3.

Table 3 Finite element solution of Problem 3

$(\frac{a}{h} = 10^5, \frac{a}{\lambda} = 10, \frac{a}{L} = 5.22, \nu = 0.3, \xi_0 = 0.522, \eta_0 = -0.738)$

$W$	$Q$	$\xi$	$\eta$
1	0.906	0.522	0.738
2	1.120	1.037	0.915
4	1.270	2.000	1.842
6	1.467	2.640	2.470

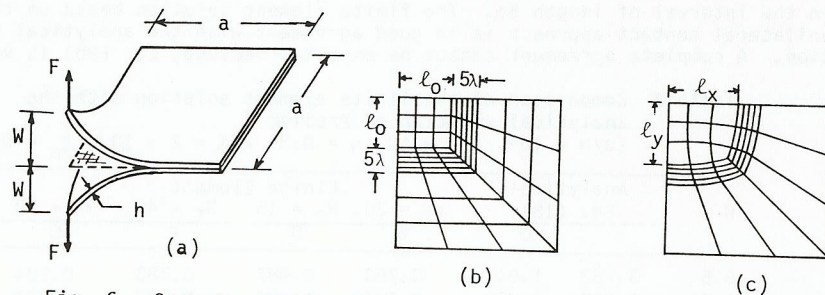


Fig. 6. Geometry and finite element mesh for the delamination of the square plate in Prob. 3

## CONCLUSIONS

The unilateral contact approach is employed to model delamination and determine the growth of the delamination. A shear deformation plate theory is used to develop a finite element model for symmetrically laminated plates which have defective bonding at the midplane. In the case of one-dimensional delamination, the fracture mechanics approach and the present approach are related and the results are compared. Application of the approach to laminated composite plates is straight forward.

## ACKNOWLEDGEMENTS

The authors express sincere thanks to Professor Ascione, University of Calabria, for his help in the solution of Problem 3. The authors are also thankful to Mrs. Charlene Christie for her patience and skilful typing of the manuscript.

## REFERENCES

- Ascione, L. and A. Grimaldi (1984). *Meccanica* (to be published).
- Duvaut, G. and J.L. Lions (1976). *Inequalities in Mechanics and Physics*, Springer-Verlag, Berlin.
- Fichera, G. (1972). *Encyclopedia of Physics*, VIa/2, Springer-Verlag, Berlin.
- Fremont, A. (1982). *Euromech Symposium on Unilateral Problems in Mechanics*, CISM-Udine, Italy.
- Grimaldi, A. and J.N. Reddy (1982). Report No. VPI-E-82-23, Virginia Polytechnic Institute and State University, Blacksburg, VA 24061.
- Reddy, J.N. (1980). *Int. J. Numer. Meth. Engrg.*, 15, 1187-1206.
- Reddy, J.N. (1984). *An Introduction to the Finite Element Method*, McGraw-Hill, New York.
- Selvadurai, A.P.S. (1979). *Elastic Analysis of Soil-Foundation Interaction*, Elsevier, Amsterdam.
- Signorini, A. (1933). *Atti della Soc. Ital. per il Progresso delle Scienze*.
- Toscano, R. and A. Maceri (1980). *Meccanica*, 15 (2), 95-106.
- Whitney, J.M. and N.J. Pagano (1970). *J. Appl. Mech.*, 37, 1031-1036.